
MAGNETISM AND FERROELECTRICITY

Magnetization Curve and Magnetic Correlations in a Nanochain of Ferromagnetic Grains with Random Anisotropy

S. V. Komogortsev and R. S. Iskhakov

Kirensky Institute of Physics, Siberian Division, Russian Academy of Sciences, Akademgorodok, Krasnoyarsk, 660036 Russia

e-mail: komogor@iph.krasn.ru

Received May 17, 2004

Abstract—The magnetization curve and magnetization correlation function are calculated for a ferromagnetic chain of single-domain nanoparticles with a randomly oriented anisotropy axis for different ratios between the exchange correlation and anisotropy energies. It is shown that the coercive force decreases as the exchange correlations increase. For strong exchange correlations, the magnetization curve is described by the following three successive magnetization processes as the applied field is increased: (i) nonuniform rotation of the magnetization of stochastic domains, (ii) collapse of the magnetic solitons, and (iii) nonuniform rotation of exchange-correlated magnetization vectors of the nanoparticles. For high fields, the calculated correlation function of the transverse magnetization components coincides with that predicted from linear theory. At low and zero fields, the main parameters of the correlation function (the variance and correlation radius) tend to certain finite values rather than diverge (as is the case in linear theory). The irreversible variation in the magnetization at low fields (the hysteresis loop) and the hysteresis of the main parameters of the correlation function are calculated. © 2005 Pleiades Publishing, Inc.

1. INTRODUCTION

The interest in simulating model systems with randomly oriented magnetic anisotropy is related to gaining a detailed understanding of the mechanisms of formation of unique magnetic properties of amorphous and nanocrystalline magnets. One of the main reasons giving rise to these properties of amorphous and nanocrystalline magnetic alloys is the randomly oriented local magnetic anisotropy coexisting with a strong exchange correlation of magnetic moments [1, 2]. Orientational randomness of anisotropy in these materials generates a specific magnetic microstructure, which can be described as an ensemble of stochastic magnetic domains. It was found that the average self-consistent characteristics of these domains (anisotropy and size) determine the main integral properties (coercivity and permeability) of amorphous and nanocrystalline magnets [3]. The stochastic magnetic domain is defined as follows. In [4], it was shown that a randomly oriented local magnetic field destroys the long-range magnetic order in a disordered ferromagnet. However, ferromagnetic ordering (correlations) is still preserved on a finite scale: due to exchange interaction, the magnetic order extends over distances that are large in comparison with interatomic distances. This ferromagnetically ordered region is a stochastic domain. To describe the magnetic structure of such systems with “intermediate” magnetic order, it is necessary to study the magnetization correlation function $K_m(r)$ [5].

The correlation function $K_m(r)$ can be directly reconstructed from experimental studies of small-angle neutron scattering in nanostructured ferromagnets [6,

7]. One of the main parameters of this function, variance $K_m(0)$, can be determined from the magnetization curve near saturation [8]. Recent studies have shown that the correlation radius R_m can also be determined from the magnetization curve [9, 10]. However, in the low-field region, perturbation theory does not apply and a linear analytical theory of the magnetization curve cannot be developed. At the same time, this region has been intensively studied experimentally and the interest in applying simulation methods to the description of nanomagnets has increased. We note a general fact: the importance of simulation experiments increases in connection with the possible description of new physical effects.

The published micromagnetic simulations deal with some applied problems of magnetism [11–16] (numerical studies of magnetization curves of a specific narrow class of materials) and some fundamental problems [17–22]. Those studies have shown that both the shape of the magnetization curve and the form of the magnetization correlation function are determined by the grain size and the fundamental magnetic constants. We believe that, in those studies, insufficient attention was paid to establishing the relation of the magnetic structure in various fields and at different relative magnitudes of exchange correlations and anisotropy to the magnetization curve of a model system, i.e., to work aimed at solving the main problem in magnetic material science of nanomagnets. Indeed, it has now become clear that the form of the magnetization correlation function $K_m(r)$ (which characterizes the spin structure) is related to the shape of the magnetization curve, $M(H)$

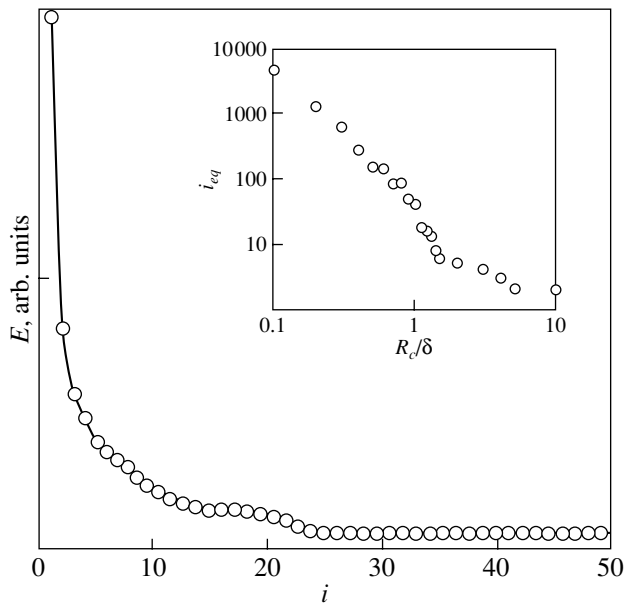


Fig. 1. Dependence of the calculated total energy of the chain on the number of iterations. The inset shows the dependence of the number of iterations required to attain the energy minimum on the parameter R_c/δ .

(which is a magnetic property of a nanomagnet). The aim of this study is to investigate simultaneously both the correlation function and the magnetization curve for a simple model system, namely, a chain of exchange-coupled nanoparticles with randomly oriented anisotropy. Our simulation is intended to provide answers to the following questions.

(1) How does the form of the magnetization curve change in the intermediate regime between weak (relative to the exchange correlation energy) and strong anisotropy?

(2) What are the features of the magnetization curve at low fields in the case of weak anisotropy?

(3) What is the character of the behavior of the correlation function of a nanostructured magnet at low fields?

The model considered is a special case of the model of a nanomagnet with one-dimensional inhomogeneities of magnetic anisotropy. However, it will be shown that this model exhibits the general laws characterizing nanomagnets. Furthermore, it is known that significant research attention has been recently turned to a new class of magnetic materials, one like magnetic nanowires. It was found that these materials are most often in the form of nanochains of exchange-bound nanoparticles [23, 24]. Therefore, our model can also be applied to describe experimental results on the magnetization of nanowires.

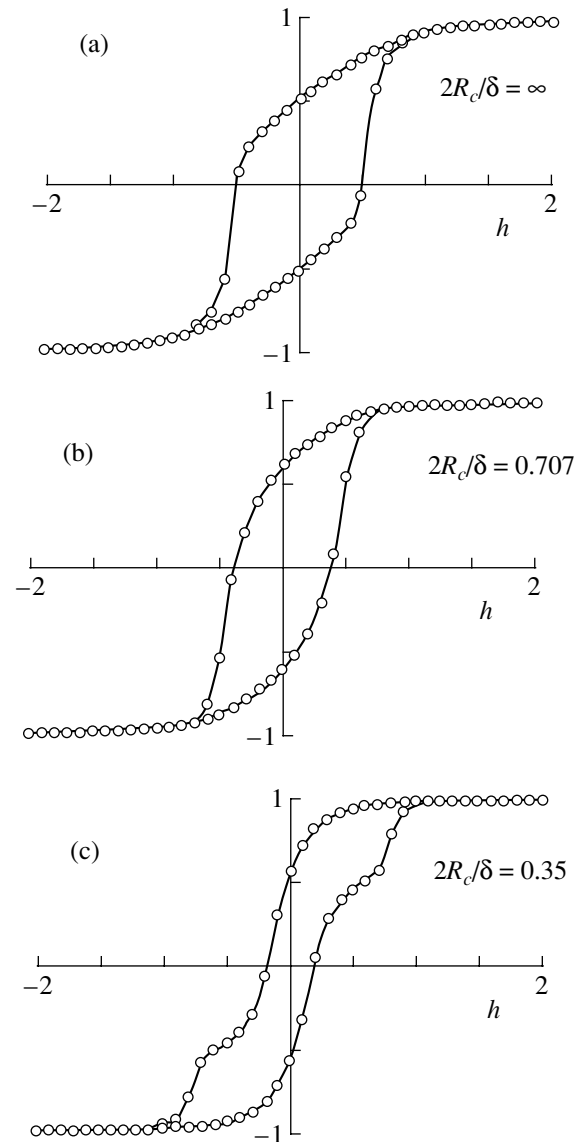


Fig. 2. Magnetization curves calculated at different values of the parameter $2R_c/\delta$.

2. METHOD AND MODEL

A discrete analog of our model is a one-dimensional chain of spins \mathbf{s} with random anisotropy at each site i with a constant nearest neighbor exchange interaction J . It is known that the energy of such a chain can be written as a sum over the sites of the chain:

$$E = - \sum_i (J\mathbf{s}_i\mathbf{s}_{i+1} + K(\mathbf{s}_i\mathbf{n}_i)^2 + H\mathbf{s}_i). \quad (1)$$

Likewise, for a nanochain of ferromagnetic grains, we can write the energy as

$$E = - \sum_i \left[\frac{1}{8} \frac{A}{R_c^2} (\cos(\theta_i - \theta_{i+1}) + \cos(\theta_i - \theta_{i-1})) + K \cos^2(\theta_i - \theta_i^a) + HM \cos \theta_i \right], \quad (2)$$

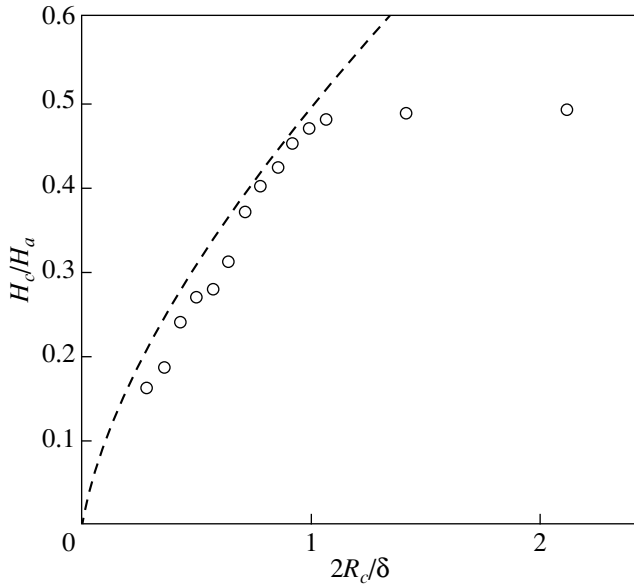


Fig. 3. The coercive force as a function of the reduced correlation radius of local anisotropy. The dashed line is the function $H_c = kH_a(2R_c/\delta)^{2/3}$.

where the direction of the local magnetization vector is characterized by the angle θ_i measured from the direction of the field \mathbf{H} ; the distance between the neighboring sites is equal to the nanoparticle size $2R_c$ (in this case, R_c is the correlation radius of random anisotropy); $A \equiv J(2R_c)^2$ is the exchange interaction constant; M_s is the saturation magnetization; $K = H_a M_s/2$ is the local magnetic anisotropy energy density, related to the anisotropy field H_a ; θ_i^a is the angle of the easy magnetization axis (a random function); and H is the external magnetic field. Since we are interested only in the states corresponding to the minimum energy, it is convenient to write Eq. (2) as

$$E = -K \sum_i \left[\frac{1}{8} \left(\frac{\delta}{R_c} \right)^2 (\cos(\theta_i - \theta_{i+1}) + \cos(\theta_i - \theta_{i-1})) + \cos^2(\theta_i - \theta_i^a) + 2h \cos \theta_i \right], \quad (3)$$

where $\delta/R_c = \sqrt{A/KR_c^2}$ is a dimensionless parameter characterizing the ratio between the exchange correlation and anisotropy energies and $h = H/H_a$. In our case (the anisotropy is random at each site), we have $R_c = 1/2$ (see, e.g., [20]). We intentionally retained the quantity R_c in Eqs. (2) and (3) in order to use, when interpreting the results, the important concept of scaling (the direct dependence of the minima of the total energy on the dimensionless parameters δ/R_c and h) in systems with random anisotropy.

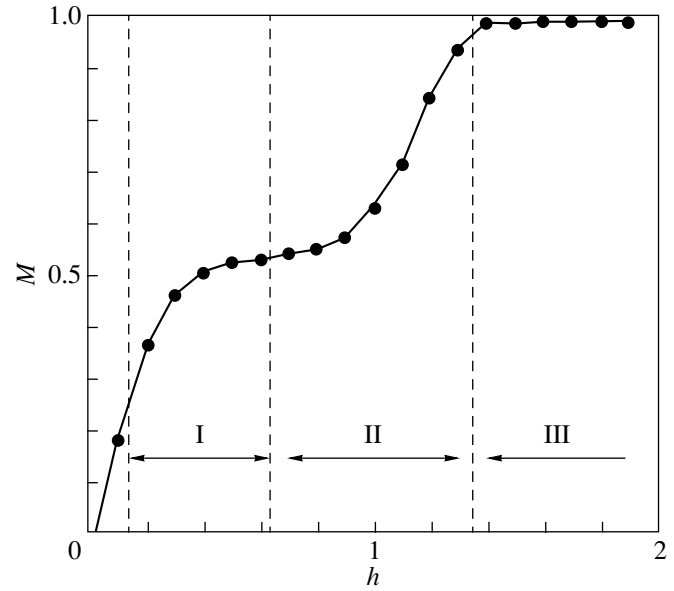


Fig. 4. Magnetization curve starting from the demagnetized state of the nanochain for the case of $R_c/\delta \approx 0.28$.

In this study, we disregard the contribution of dipole–dipole interaction to the total energy for several reasons. First, in earlier simulations of similar systems [11, 12], it has been shown that the magnetic structure and the magnetization curve of nanomagnets only weakly depend on the magnetic dipole interactions, in contrast to those of large-grain and single-crystal ferromagnets. This result is qualitatively clear, since only exchange correlations and magnetic anisotropy participate in the formation of the basic unit of the spin structure, the stochastic magnetic domain. Second, the inclusion of long-range magnetic dipole forces

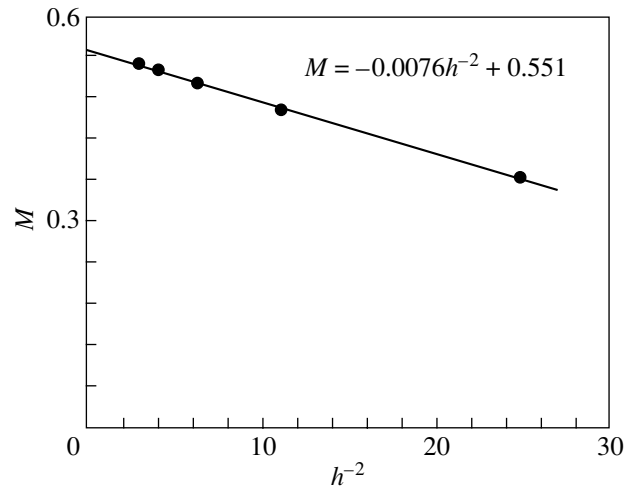


Fig. 5. Magnetization curve in the first field range ($R_c/\delta \approx 0.28$).

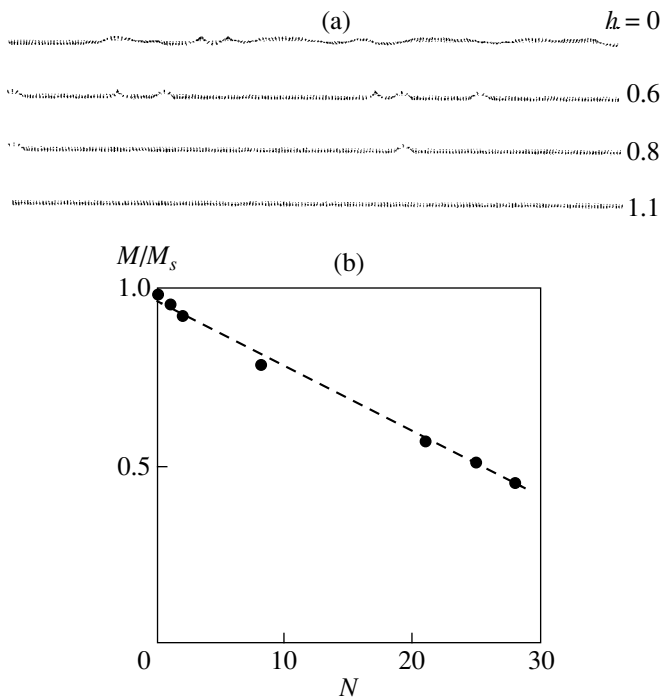


Fig. 6. (a) Magnetic structure of a fragment of the chain at different values of the external field in the second range. (b) Dependence of magnetization on the number of magnetic solitons in the second field range.

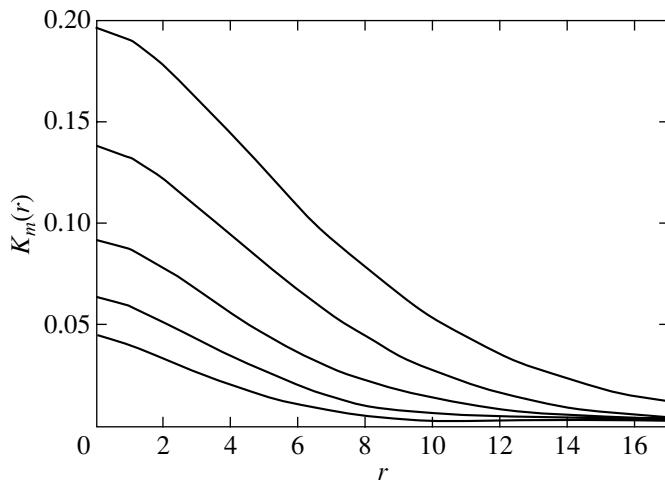


Fig. 7. Dependence of the correlation function for the transverse magnetization components on the external field (from top to bottom: $h = 0, 0.1, 0.2, 0.3, 0.4$) for $2R_c/\delta = 0.35$.

increases the amount of computational time required (which is long even if we disregard these forces) by orders of magnitude.

There are two different methods for solving our problem numerically: (i) numerical solution of the differential equation obtained by minimizing functional (2) or (3) [18–20] and (ii) a straightforward choice of the

spin distribution corresponding to the minimum of total energy (2) or (3) (see, e.g., [17]). The advantage of the first method in the case of $R_c/\delta \ll 1$ (strong exchange correlations, weak anisotropy) is that the computation speed is high, in contrast to the second method, where the computation time increases sharply with decreasing ratio R_c/δ (see inset to Fig. 1). In the case where R_c/δ is of the order of unity or larger (strong anisotropy, weak exchange correlations), the first method fails, since the system becomes strongly nonlinear and divergences appear when the differential equation is solved numerically. Moreover, the solution to the differential equation is assumed to be unique and, therefore, cannot be used at low fields, where hysteresis arises. In this case, the problem is solved using the second method.

A procedure for calculating the magnetization curve using the first method was suggested and described in [18, 19]. With the second method, the magnetization curve can be found as follows: for a certain field (e.g., $H = 0$), “relaxation” of the system is performed (by choosing the magnetization distribution that corresponds to the minimum energy), then the field is varied slightly and relaxation from the previous state is performed. We assume that this procedure allows one to reach the local energy minima responsible for hysteresis.

The relaxation is performed as follows. The angle θ_i at site i is changed by Δ , and the energy at this site is calculated. If the energy increases as compared to the previous state, the state is not stored in memory and the angle is changed by $-\Delta$; this procedure is repeated with a subsequent decrease in the step to ± 0.0001 rad. This procedure is performed successively for each site.

Due to the coupling between the nearest neighbors, the state at site i is changed when minimizing the energy at site $i + 1$. Therefore, to minimize the energy, we have to come back and perform the relaxation at site i again. By performing such iterations for the entire chain, we found that the total energy first decreases and then ceases to vary at a certain stage (Fig. 1). We assume that this state corresponds to the energy minimum. We note that the choice of another sequence of step-by-step spin relaxation can result in a different random distribution of magnetization; however, for a sufficiently long chain, the average characteristics do not change. In the calculations, we used chains 1000- to 5000-spins long and periodic boundary conditions. Since the energy of a nanochain is invariant under rotations in the plane normal to the external field, we averaged over the angle in this plane when averaging the projection of the magnetization onto the field axis.

3. RESULTS AND DISCUSSION

Figure 2 shows the magnetization curves calculated for different values of the parameter $2R_c/\delta$ characterizing the ratio between the anisotropy and exchange correlation energies. The curve in Fig. 2a corresponds to

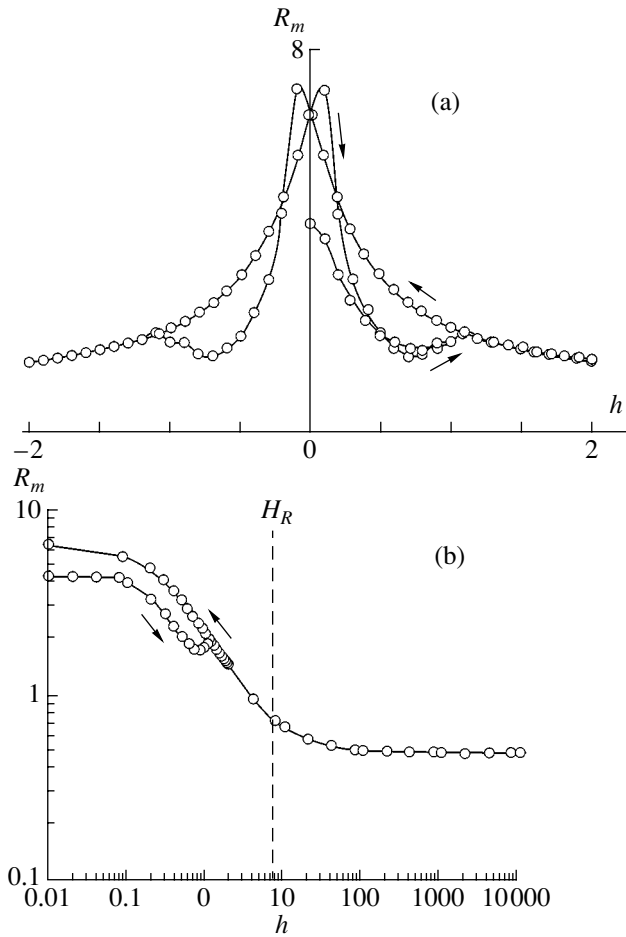


Fig. 8. Field dependence of the magnetization correlation radius R_m on (a) a linear and (b) a logarithmic scale (for $2R_c/\delta = 0.35$).

zero exchange correlation energy and reproduces the classical result of Stoner and Wohlfarth for a system of noninteracting single-domain particles (or very large crystallites, with $R_c \gg \delta$) with random easy-axis anisotropy [25]. In this case, the coercive field is $h_c = 1/2$ ($H_c = H_a/2$) and the residual magnetization is $M_r = (1/2)M_s$. The coercive force decreases with decreasing $2R_c/\delta$, i.e., as exchange correlations are included (Figs. 2b, 2c). The dependence of H_c on $2R_c/\delta$ obtained from the calculated magnetization curves is plotted in Fig. 3. In the region of $2R_c/\delta < 1$, the calculated dependence of the coercive force becomes close to the analytical dependence of the average anisotropy field of a one-dimensional magnetic block (stochastic magnetic domain) [18, 26, 27]:

$$\langle H_a \rangle = H_a (2R_c/\delta)^{2/3}. \quad (4)$$

By comparing the curves in Fig. 3, we see that H_c as a function of $2R_c/\delta$ follows the same power law as does $\langle H_a \rangle$ and that these quantities differ by a constant factor, $H_c = k\langle H_a \rangle$. In our case, $k \approx 0.48$. This correlation between the dependences of H_c and $\langle H_a \rangle$ corresponds to

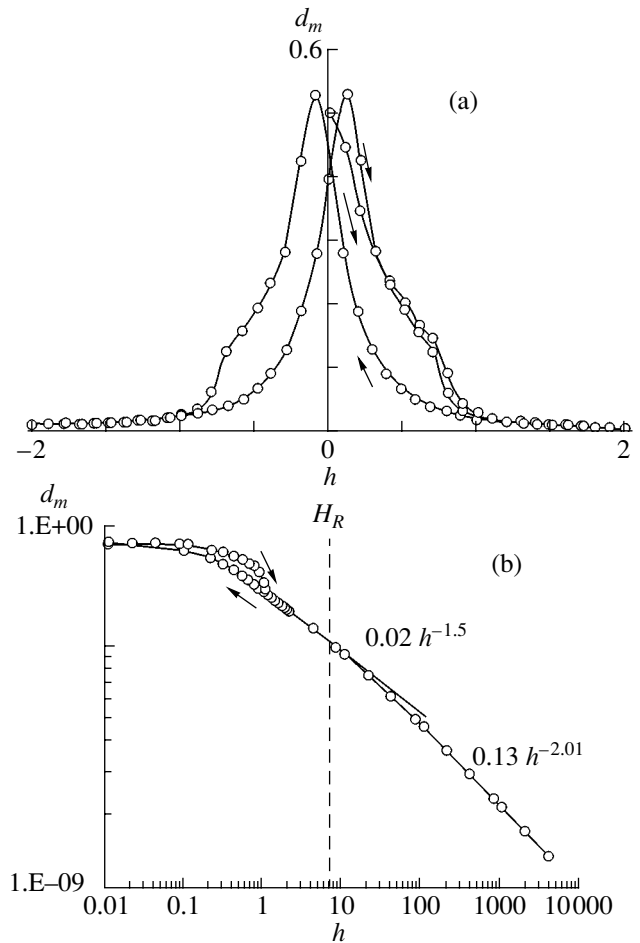


Fig. 9. Field dependence of the magnetization variance $d_m = K_m(0)$ on (a) a linear and (b) a logarithmic scale (for $2R_c/\delta = 0.35$).

a model in which the magnetic structure of the nanochain is considered a system of exchange-uncoupled magnetic blocks with randomly oriented anisotropy axes averaged over each block.

For strong exchange correlations, a steplike feature arises on the magnetization curve (Figs. 2c, 4). This feature appears at $2R_c/\delta \approx 0.4$ and becomes more pronounced at stronger exchange correlations ($2R_c/\delta \ll 1$). In Fig. 4, we show the calculated magnetization curve starting from the demagnetized state of the nanochain for the case of $2R_c/\delta \approx 0.28$. We see that this magnetization curve can be divided into three parts, corresponding to three field ranges.

In the first range, the magnetization increases with field due to nonuniform rotation of the magnetizations of stochastic domains. This interpretation is confirmed by the fact that the $M \sim H^{-2}$ dependence is satisfied in this region (Fig. 5). We note that this dependence was predicted and observed experimentally in [10]. The average anisotropy field $\langle H_a \rangle$ of a block determined from the Akulov low-field dependence agrees well with the value of $\langle H_a \rangle$ calculated from Eq. (3).

In the second field range of the $M(h)$ curve, the magnetic structure proves to be an ensemble of magnetic blocks with the average magnetizations oriented along the field and an additional ensemble of localized regions in which the magnetization is not reversed; these regions are topological magnetic solitons whose structure and size do not depend on the external field within the second range (Fig. 6a). As the field increases, the magnetization of magnetic solitons is reversed in a jumplike manner and the solitons decrease in number and disappear in fields above H_a ($h > 1$). Figure 6b shows the dependence of the magnetization on the number of magnetic solitons in the second field range. The linear dependence indicates that the magnetization reversal in each soliton provides an equal contribution to the increase in magnetization. Since the solitons do not differ in size or magnetization in the second range, we may consider them as a sort of magnetization quanta.

The magnetic structure of the nanochain in the third field range of the reversible $M(h)$ dependence is a stochastic magnetic structure or "magnetization ripples" (see, e.g., [28]). This structure is described well by the one-dimensional linear theory of reversible processes of inhomogeneous magnetization rotation [29].

We calculated the correlation function for the transverse components of magnetization for each magnetic state of the nanochain corresponding to a point on the calculated hysteresis loop (for $2R_c/\delta \approx 0.35$). Figure 7 shows the $K_m(r)$ dependence calculated for different fields. The main parameters of the function $K_m(r)$ are the variance $d_m = K_m(0)$ and the correlation radius R_m . We see that both the variance $K_m(0)$ and the magnetic correlation length $2R_m$ decrease with increasing external field. For our simple model, the field dependences of $d_m = K_m(0)$ and $R_m(h)$ can be calculated in the entire field range.

Figures 8 and 9 show the calculated field dependences of the correlation radius $R_m(h)$ and the variance of the transverse components of magnetization $d_m(h)$ plotted on both linear and logarithmic scales. We see that the h dependences of the main parameters of the correlation function $K_m(r)$, as well as the $M(h)$ dependence, are characterized by a region of reversible variation and a region of irreversible changes (hysteresis). The reversible variations in $R_m(h)$ and $d_m(h)$ are the simplest to explain. At high fields, the calculated R_m and d_m are identical to those predicted from linear theory (Figs. 8b, 9b). Indeed, according to linear theory [29], in fields below $H_R = 2A/M_s R_c^2$, we have $R_m = \sqrt{2A/M_s H} \equiv \delta h^{-1/2}$ and $d_m = (aH_a)^2 H_R^{-1/2} H^{-3/2} = a^2(R_c/\delta)h^{-3/2}$. In fields above H_R , R_m tends to a constant value, which is approximately equal to the correlation radius of random magnetic anisotropy ($R_c = 1/2$ in our case), and the variance of magnetization behaves as $d_m = (aH_a)^2 H^{-2} = a^2 h^{-2}$. It is seen in Figs. 8b and 9b that the calculated functions

$R_m(h)$ and $d_m(h)$ exhibit similar behavior. We note that these results were obtained both by directly minimizing the total energy (in the present work) and by solving the corresponding differential equation (in [30]).

The irreversible variations in $R_m(h)$ and $d_m(h)$ are most difficult to explain. We see that, as the field approaches zero, the quantities R_m and d_m do not diverge (contrary to the predictions from linear theory) but rather tend to finite values. The variations in $R_m(h)$ and $d_m(h)$ with field are hysteretic. We point out specific features of this hysteresis. First, we see that $R_m(0)$ in the demagnetized state is smaller than $R_m(0)$ in the state with residual magnetization (the opposite is true for $d_m(0)$). Second, we see that there is a field range (close to $h = 1$) where $R_m(h)$ increases with H , in disagreement with the prediction from linear theory. We note that this field range coincides with the region where magnetic solitons exist and a specific feature arises on the magnetization curve (the second range).

The behavior of $R_m(h)$ and $d_m(h)$ in the field range $h < 1$ ($H < H_a$) allows us to assert that the quantitative characteristics of a stochastic domain (its size and average anisotropy) are fairly arbitrary in many respects (at least, in the one-dimensional case). Therefore, these quantities can only be evaluated by order of magnitude.

Thus, in our simulation we succeeded in providing answers to all three questions stated in Section 1.

ACKNOWLEDGMENTS

This study was supported by the Krasnoyarsk Regional Science Foundation (grant no. 12F0011C), the Russian Foundation for Basic Research (grant no. 04-02-16230), and the Governmental Support Foundation (grant no. MK-1684.2004.2).

REFERENCES

1. V. A. Ignatchenko and R. S. Iskhakov, Zh. Éksp. Teor. Fiz. **72**, 1005 (1977) [Sov. Phys. JETP **45**, 526 (1977)].
2. R. Alben, J. J. Becker, and M. C. Chi, J. Appl. Phys. **49**, 1653 (1978).
3. G. Herzer, IEEE Trans. Magn. **26**, 1397 (1990).
4. Y. Imry and S.-K. Ma, Phys. Rev. Lett. **35**, 1399 (1975).
5. J. M. Ziman, *Models of Disorder: The Theoretical Physics of Homogeneously Disordered Systems* (Cambridge Univ. Press, London, 1979; Mir, Moscow, 1982).
6. J. Weissmuller, A. Michels, J. G. Barker, A. Wiedemann, U. Erb, and R. D. Shull, Phys. Rev. B **63**, 214414 (2001).
7. A. Michels, R. N. Viswanath, J. G. Barker, R. Birringer, and J. Weissmuller, Phys. Rev. Lett. **91**, 267204 (2003).
8. V. A. Ignatchenko, R. S. Iskhakov, and G. V. Popov, Zh. Éksp. Teor. Fiz. **82**, 1518 (1982) [Sov. Phys. JETP **55**, 878 (1982)].
9. R. S. Iskhakov, S. V. Komogortsev, Zh. M. Moroz, and E. E. Shalygina, Pis'ma Zh. Éksp. Teor. Fiz. **72**, 872 (2000) [JETP Lett. **72**, 603 (2000)].

10. R. S. Iskhakov, V. A. Ignatchenko, S. V. Komogortsev, and A. D. Balaev, Pis'ma Zh. Éksp. Teor. Fiz. **78**, 1142 (2003) [JETP Lett. **78**, 646 (2003)].
11. H. Kronmuller, R. Fischer, M. Seeger, and A. Zern, J. Phys. D: Appl. Phys. **29**, 2274 (1996).
12. R. Fischer and H. Kronmuller, J. Magn. Magn. Mater. **184**, 166 (1998).
13. J. Fidler and T. Schrefl, J. Magn. Magn. Mater. **203**, 28 (1999).
14. W. M. Saslow and N. C. Koon, Phys. Rev. B **49**, 3386 (1994).
15. O. Nedelko, P. Dikukh, and A. Slawska-Waniewska, J. Magn. Magn. Mater. **254–255**, 281 (2003).
16. I. R. McFadyen and I. A. Beardsley, J. Appl. Phys. **67**, 5540 (1990); I. A. Beardsley and J. S. Zhu, J. Appl. Phys. **67**, 5352 (1990).
17. R. Dickmann and E. M. Chudnovsky, Phys. Rev. B **44**, 4397 (1991).
18. A. A. Ivanov, V. A. Orlov, and G. O. Patrushev, Fiz. Met. Metalloved. **84** (2), 47 (1997) [Phys. Met. Metallogr. **84**, 125 (1997)].
19. A. A. Ivanov and G. O. Patrushev, Fiz. Met. Metalloved. **86** (4), 1 (1998) [Phys. Met. Metallogr. **86**, 331 (1998)].
20. A. A. Ivanov, V. A. Orlov, and G. O. Patrushev, Fiz. Tverd. Tela (St. Petersburg) **41**, 1432 (1999) [Phys. Solid State **41**, 1311 (1999)].
21. B. Dieny and B. Barbara, Phys. Rev. B **41**, 11549 (1990).
22. D. R. Denholm and T. J. Sluckin, Phys. Rev. B **48**, 901 (1993).
23. H. Zeng, R. Skomski, L. Menon, Y. Liu, S. Bandyopadhyay, and D. J. Sellmyer, Phys. Rev. B **65**, 134426 (2002).
24. R. S. Iskhakov, S. V. Komogortsev, A. D. Balaev, A. V. Okotrub, A. G. Kudashov, V. L. Kuznetsov, and Yu. V. Butenko, Pis'ma Zh. Éksp. Teor. Fiz. **78**, 271 (2003) [JETP Lett. **78**, 236 (2003)].
25. E. C. Stoner and E. P. Wohlfarth, Philos. Trans. R. Soc. London, Ser. A **240**, 599 (1948).
26. R. S. Iskhakov, S. V. Komogortsev, A. D. Balaev, and L. A. Chekanova, Pis'ma Zh. Éksp. Teor. Fiz. **72**, 440 (2000) [JETP Lett. **72**, 304 (2000)].
27. R. Skomski, J. Phys.: Condens. Matter **15**, R841 (2003).
28. V. A. Ignatchenko, Zh. Éksp. Teor. Fiz. **54**, 303 (1968) [Sov. Phys. JETP **27**, 162 (1968)].
29. V. A. Ignatchenko and R. S. Iskhakov, Fiz. Met. Metalloved., No. 6, 75 (1992).
30. A. V. Luk'yanenko and S. V. Komogortsev, in *Proceedings of the II Baikal International Conference on Magnetic Materials* (Irkutsk, 2003), p. 72.

Translated by I. Zvyagin